Chalcogenide Letters

Tech Science Press

http://doi.org/10.32604/cl.2026.081302

ARTICLE

Annealing-Induced Structural and Optical Modifications in SnS Thin Films and Their Impact on CO_2 Gas Sensing Performance

Seham Hassan Salman[1], Sarmad Mahdi Ali[1], Hawraa Hadi[2,*] and Dhufr Hadi[3]

[1]Department of Physics, College of Education for Pure Science (Ibn-Alhaitham), University of Baghdad, Baghdad, Iraq
[2]Department of Anesthesia, College of Health and Medical Techniques/Kufa, Al-Furat Al-Awsat Technical University, Al-Kufa, Iraq
[3]Department of Physics, College of Education for Pure Sciences, University of Kerbala, Karbala, Iraq
*Corresponding Author: Hawraa Hadi. Email: hawraaalwaelly@gmail.com or hawra.jiyadckm@atu.edu.iq

Received: 27 February 2026; Accepted: 05 May 2026; Published: 02 June 2026

ABSTRACT: Films of (SnS) with a thickness of 400 nm were deposited by the thermal evaporation technique to investigate the influence of annealing temperature on their Physics and CO_2 gas-sensing characteristics. The deposited films were annealed at 200, 300, and 400°C. Structural characterization was performed using XRD, and the obtained results revealed that all samples possessed an orthorhombic crystal structure with a preferred orientation (301). The annealing treatment significantly improved the crystallinity of the films and reduced structural defects and lattice strain. Surface morphology investigations were performed using atomic force microscopy (AFM), which revealed noticeable modifications in grain size distribution, surface roughness, and film homogeneity after annealing. Optical characterization was conducted in the range of 300–1100 nm. The optical band gap values were determined using the Tauc method from the $(\alpha h\nu)^2$ versus $h\nu$ plots and were found to be 1.35, 1.38, 1.62, and 1.40 eV for the as-deposited, 200, 300, and 400°C annealed samples, respectively. Several optical constants, such as the absorption, extinction coefficient, and refractive index, were also evaluated. Furthermore, the CO_2 gas-sensing performance of the SnS thin films was examined at operating temperatures of 50, 100, and 150°C. The results demonstrated that both annealing temperature and operating temperature strongly affected the sensitivity and response behavior of the films. Enhanced sensing performance was attributed to improvements in crystallinity, surface morphology, and charge transport properties induced by annealing. The obtained results suggest that annealed SnS thin films are promising candidates for optical and gas-sensing applications.

KEYWORDS: SnS thin films; annealing; gas sensor and operating temp.

1 Introduction

Due to their unique physical and chemical properties, tin sulfide (SnS) thin films are important semiconductor materials in scientific research, making them suitable for applications such as solar cells, sensors, and microelectronic devices. Zinc sulfide films possess a suitable band gap in the visible and near-infrared spectral ranges, and their non-toxicity and availability make them a suitable choice for applications requiring efficient and economical thin-film materials. Thermal annealing after thin film deposition is one of the most important mechanisms for controlling the physics properties of a material [1,2].

Annealing affects the crystalline structure of the films, improving crystal arrangement and reducing lattice defects. This, in turn, affects the optical band gap and other optical values such as transmittance and absorption. Additionally, it alters the electrical band gap, which in turn changes the electrical conductivity and charge carrier concentration [3,4].

Annealing affects the structural, optical, and electrical properties of tin sulfide thin films, improving their performance in applications such as gas sensors and solar cells. Patel et al. prepared SnS thin films using spray deposition and studied the effect of annealing, finding that increasing annealing temperature improved crystallinity and significantly modified the optical properties of the films [5]. Similarly, Zgair and colleagues studied the preparation of tin sulfide films by evaporation and their annealing at 200°C, finding that annealing improved the structural and optical properties [6]. Zgair et al. (2023) also investigated the effect of annealing on the properties of tin sulfide films and the formation of mixed phases such as SnS–SnO_2 as a result of partial oxidation, which affects their surface properties. This effect is important for gas sensing applications [7]. Recent studies have indicated the potential use of SnS in gas sensing applications due to its electronic properties and strong interaction with gas molecules [8]. This work aims to investigate the effect of different annealing temperatures on the structural, morphological, and optical properties of SnS thin films prepared by thermal evaporation and to correlate these changes with their behavior in carbon dioxide gas sensing.

2 Experiments

Tin and sulfur were mixed in a 1:1 ratio to form an alloy, then heated at 1100°C for four hours to obtain a homogeneous melt, and then cooled. The alloy was removed from the tube, ground, and a portion was used to prepare 400 nm thin films by thermal evaporation on thoroughly cleaned glass substrates (the substrates were washed with distilled water to remove dust and suspended impurities. They were then ultrasonically cleaned in a detergent solution for 15 min to remove organic impurities and grease. The substrates were then washed several times with distilled water and ultrasonically cleaned in ethanol for ten minutes to remove any remaining organic residues. Finally, the substrates were washed again with distilled water, dried, and then stored in a dust-free environment until use). The system was evacuated to a pressure of 3×10^{-8} bar. The distance between the substrate and the tube was 18 cm. The deposition rate was 0.81 nm/s. The thermally prepared films were cured at temperatures of 200, 300 and 400°C for one hour using an electric oven.

The structural characteristics of SnS films and lattice constant are tested by the XRD device model (Shimadzu—XRD 600, Shimadzu company, Japan), XRD with a Cu-Kα radiation source (0.15406 nm) turned on at 30 mA and 40 kV. The specimens were tested from 10° to 80°.

To study the morphology of film by the AFM. In the range of wavelengths (300–1100) nm, a to measure the optical properties, a UV-Vis spectrometer (UV-1650 Shimadzu) was used. Finally, the SnS gas sensor was fabricated by depositing aluminum conductive electrodes onto prepared and annealed films. The film's sensitivity to gas is measured by the change in the film's resistance when exposed to carbon dioxide gas at different operating temp.

3 Results and Discussion

3.1 X-Ray Diffraction

Fig. 1. shows the XRD of the thin films before and after annealing at (200–300 and 400)°C for 1 h. The figure indexed peaks such as (210), (301), (311), (202), (212), and (711) are characteristic peaks of the orthorhombic structure of the SnS, according to JCPDS standard card (PDF Card No. 39-0354). The strongest peak is often located around $2\theta \approx 31–32°$. It reverts to the (301) or (210) plane depending on the peak intensity and growth direction. This confirms the formation of a polycrystalline SnS phase without distinct secondary phases such as SnS_2 or Sn_2S_3, especially at higher annealing temperatures.

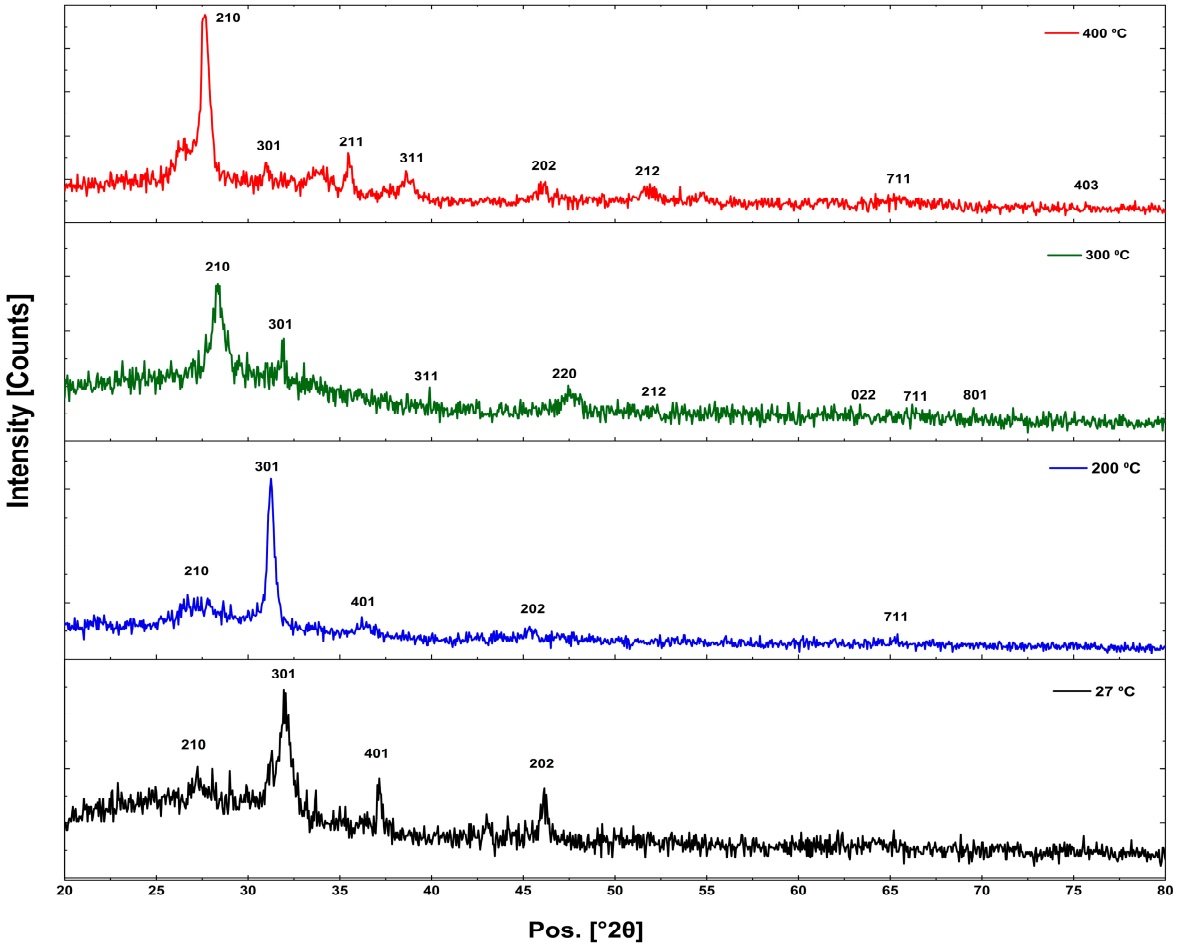

Figure 1: XRD of SnS thin films: before and after annealing.

Using the Shearer equation to calculated the size of the crystals (D) [9]:

$$D = \frac{k\lambda}{\beta \cos\theta} \tag{1}$$

where: β (rad) represents the full width at half maximum, θ symbolizes the Bragg angle and k is a Scherrer constant (k = 0.94). Eq. (2) can be used to find the density of the dislocations (δ) [10]:

$$\delta = \frac{1}{D^2} \tag{2}$$

The microstress (ε) of thin films of tin sulfide was found using the formula [11].

$$\varepsilon = \frac{\beta \cos\theta}{4} \tag{3}$$

XRD results in Table 1 for SnS films show that grain size does not increase linearly with increasing temperature but rather is influenced by a balance between several physical processes. Initially, as the annealing temperature increases from the unannealed state to moderate temperatures (200–300)°C, there is an increase in the atomic diffusion energy of atoms within the crystal lattice, allowing them to move

towards more ordered positions and reducing defects and cracks. This typically leads to an increase in grain size and improved crystallinity due to the merging of smaller grains and a reduction in high-energy grain boundary regions [12]. However, at higher temperatures within this range, recrystallization, or a change in preferred crystallization orientation, may occur, rearranging the grains and forming new, smaller grains with different surface energies. Annealing not only leads to grain growth but also to the reorganization of the structural composition at certain temperatures. Therefore, the crystal size decreases at that temperature, and sulfur atoms are lost at high annealing temperatures (400°C). The competition between recrystallization, atomic diffusion, and surface energy equilibrium forces the fluctuation in grain size with increasing annealing temperature of tin sulfide films [13,14].

Table 1: The data of XRD analysis and the structure parameters of SnS thin films.

Samp.	2θ XRD	2θ AST.	D (nm)	$\delta \times 10^{14}$ (Line/nm^2)	ε	dXRD.	dAst.	hkl
As-dep.	32.003	31.712	9.18	0.00377	0.0119	2.794	2.819	301
200°C	31.266	31.712	17.96	0.00193	0.0031	2.858	2.819	301
300°C	28.391	27.051	7.18	0.00483	0.0194	3.141	3.294	210
400°C	27.685	27.051	14.52	0.00239	0.0047	3.220	3.293	210

3.2 Morphology

Figs. 2 and 3 (AFM) images of tin sulfide films show that the film surface consists of tightly packed nanoparticles with an irregular distribution, characterized by clear peaks and protrusions separated by depressions, confirming the polycrystalline nature of the film. This is consistent with XRD. This is consistent with the study [13]. The images also show variations in grain size and surface density among the samples. This variation is attributed to the annealing effect, which promotes surface diffusion and recrystallization, leading to the merging of small grains and the formation of larger ones [12]. Furthermore, increasing the temperature leads to a decrease in the number of grain boundaries due to their growth, which in turn reduces dispersion centers and improves electrical conductivity, as reported by [15]. The agglomeration pattern observed in the images is explained by the Volmer–Weber island growth mode, where primary nuclei form and then gradually grow and merge to form a continuous layer—a mechanism common in polycrystalline SnS films [14]. Additionally, increased surface roughness leads to an increase in the effective surface area and adsorption sites, which improves the response of the films in gas sensing applications, consistent with what has been reported in the literature on p-type semiconductor sensors [13].

3.3 Optical Properties

The transmittance spectra of SnS thin films before and after annealingin Fig. 4 shows very low values in the UV-Vis and visible regions due to strong absorption of high-energy (UV) photons. This is normal because the photon energy is greater than the energy gap (E_g) (~1.3–1.5 eV). This is consistent with previous studies [16]. A gradual increase in transmittance is observed at higher wavelengths (NIR). This behavior is attributed to the decrease in photon energy at longer wavelengths. Furthermore, the decrease in transmittance with increasing annealing temperature is associated with improved crystallinity, increased grain size, and enhanced light scattering at grain boundaries. This is consistent with previous studies [17].

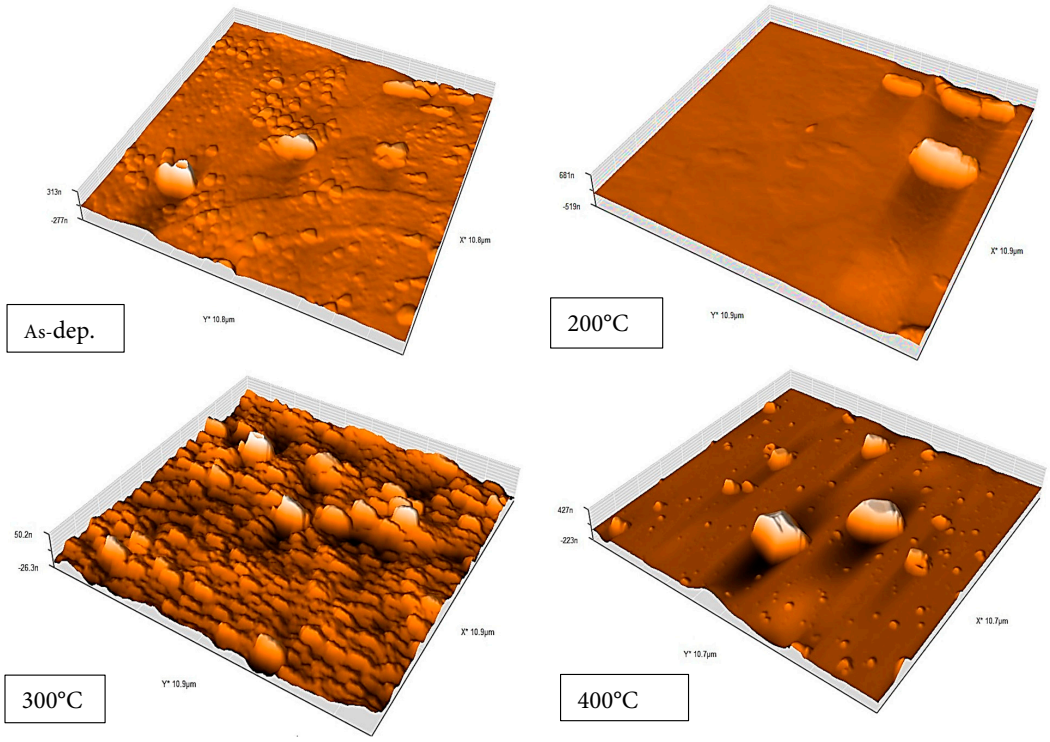

Figure 2: Image AFM—3D for thin film before and annealing.

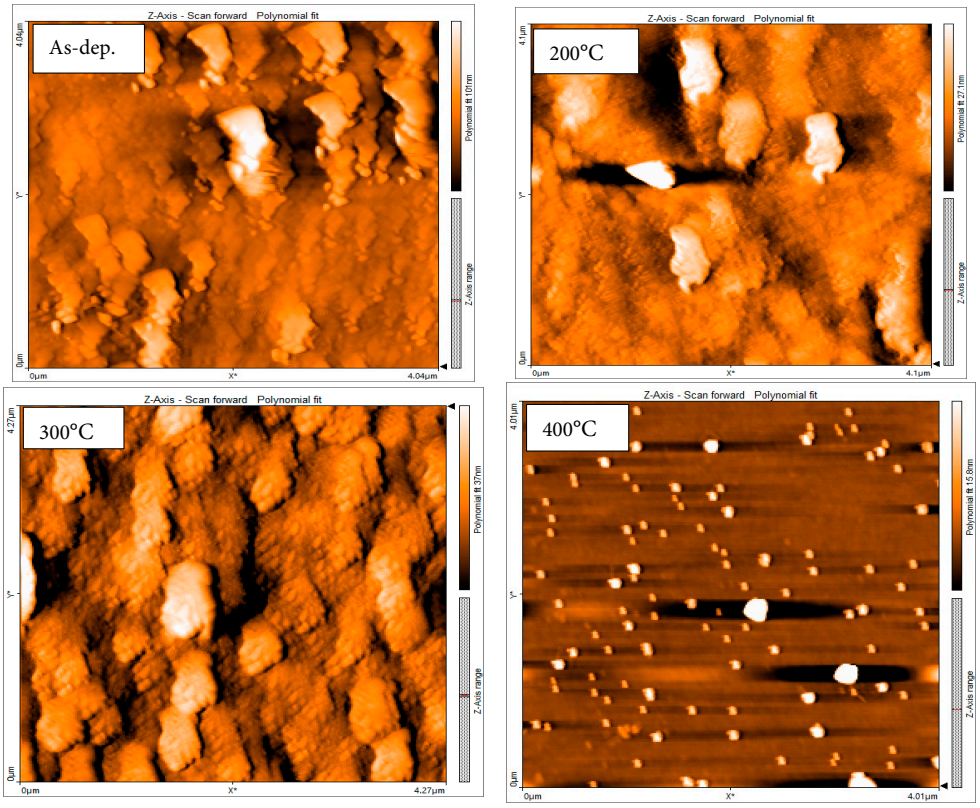

Figure 3: Image AFM—2D for thin film before and annealing.

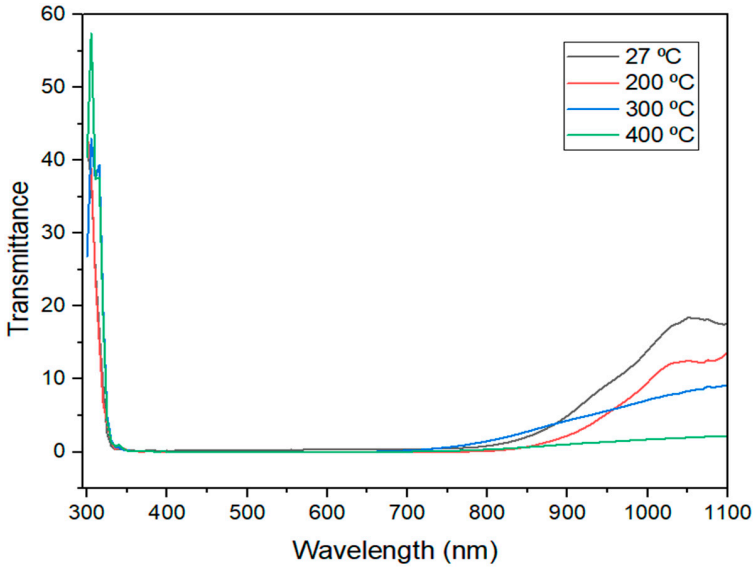

Figure 4: Transmission of films before and after annealing.

Fig. 5 shows the reflectance of annealed and unannealed SnS films. High values are observed in the ultraviolet region, followed by a decrease in the visible light range due to strong photoabsorption. At longer wavelengths, reflectance increases as the photon energy falls below the bandgap energy. The change in reflectance with annealing temperature is attributed to variations in crystallinity, grain size, and surface shape. The film annealed at 300°C exhibits the lowest reflectance, indicating increased photo absorption, which is consistent with previous studies [18].

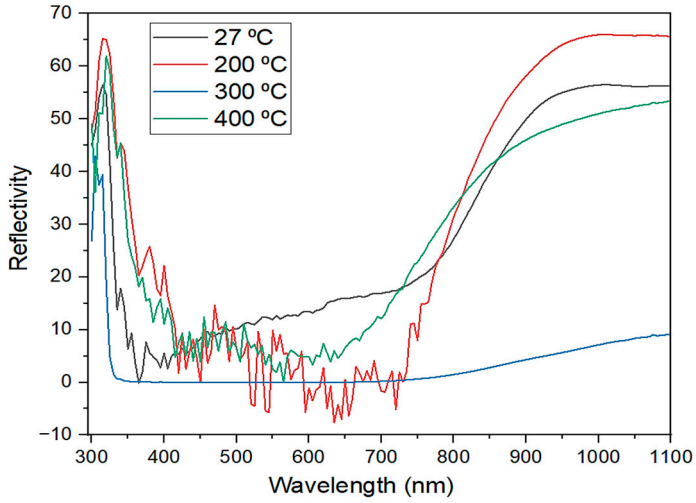

Figure 5: Reflectivity for SnS thin film as-deposited and annealed.

The absorption coefficient (α) of tin sulfide films was found by formula [10].

$$\alpha = \frac{2.303\ A}{t} \tag{4}$$

The absorption coefficient was found to be 10^4 cm^{-1}, as shown in Fig. 6.

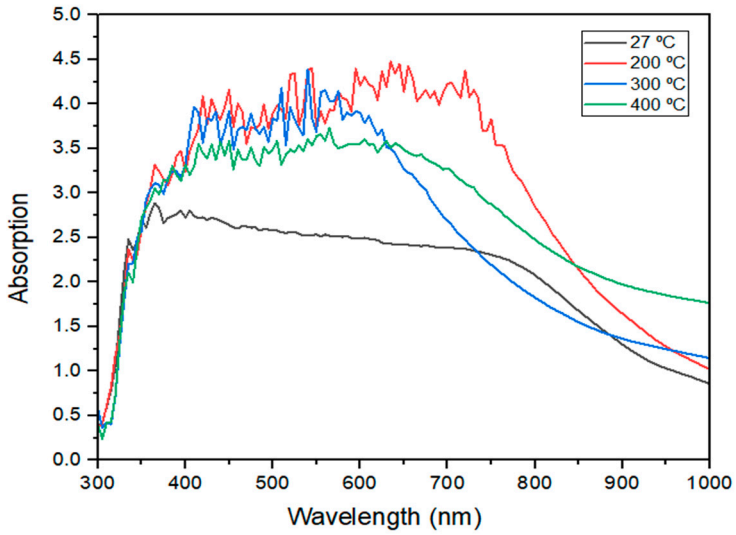

Figure 6: Absorption coefficient for thin film before and annealing.

Fig. 7 represents Extinction coefficient (K) of tin sulfide films before and after annealing at (200, 300, and 400)°C.

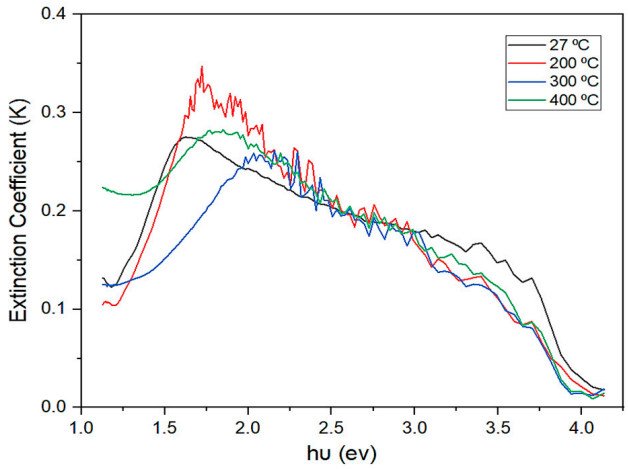

Figure 7: Extinction coefficient for thin film before and annealing.

The extinction coefficient, K, is directly related to the material's ability to absorb light and is given by the equation [10]:

$$K = \frac{\alpha\lambda}{4\pi} \tag{5}$$

The extinction coefficient in SnS increases near the energy gap due to direct electron transitions. The highest value at 200°C indicates improved optical properties. The decrease in k at high energies indicates the end of the strong absorption band. The curve behavior confirms that annealing directly affects the electronic structure and optical density [17].

The band gap (E_g) can be determined by equation [18],

$$\alpha h\nu = \mathrm{B}\left(h\upsilon - E_g\right)^n \tag{6}$$

The band gap of the films was determined by plotting $(\alpha h\nu)^2$ versus $h\nu$ from Fig. 8. E_g = 1.35 eV was found for the films before annealing, and the E_g increased with increasing annealing temp.

This increase in the energy gap can be explained by the fact that annealing improves the crystallinity of the films, which reduces the structural defects that usually cause the appearance of tails in the band structure (Aurbach tails).

Additionally, heat treatment can induce minor changes in the chemical composition of the thin film, particularly the re-evaporation of sulfur at higher temperatures, which can alter the electronic structure and charge carrier concentration. These structural modifications can contribute to band structure rearrangements and a widening of the band gap. This is agreed with the findings of researchers [5,19].

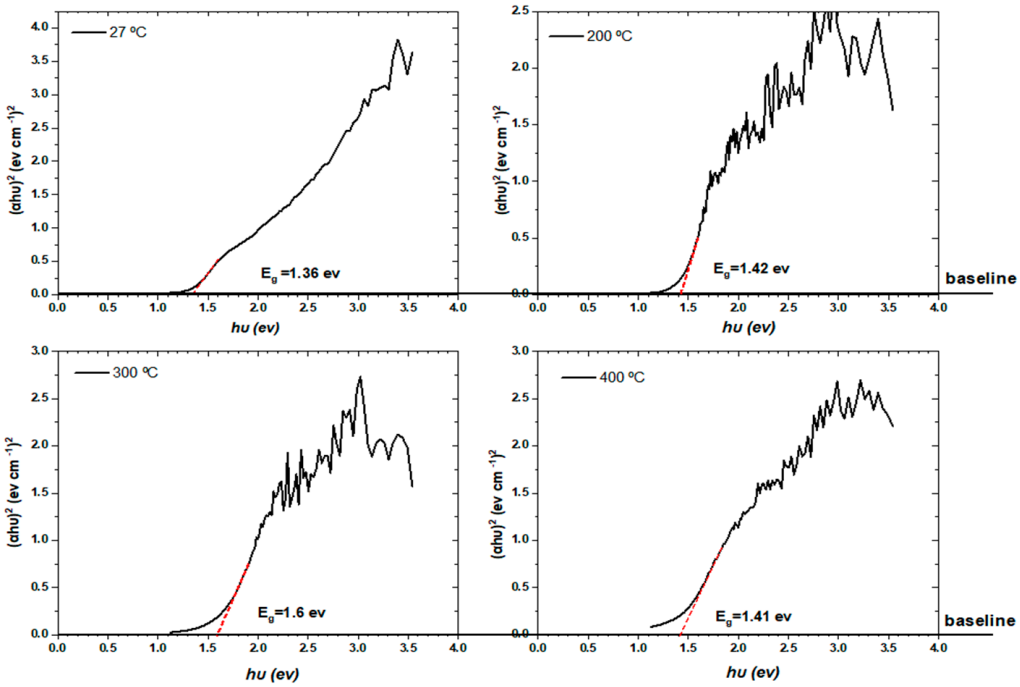

Figure 8: $(\alpha h\nu)^2$ vs. $h\nu$ plots for films before and annealed at (200, 300 and 400)°C.

3.4 Sensing Properties

The Figs. 9–12 illustrate the change in resistance over time for the films before and after annealing and several different operating temperatures (50, 100 and 150)°C. It was found that resistance decreases when exposed to carbon dioxide gas, and this proves that the SnS films are of the p-type. Carbon dioxide (CO_2) is a gas with weak oxidizing behavior when it reacts with semiconductor surfaces. When tin sulfide films, which often exhibit p-type semiconducting behavior, are exposed to CO_2, adsorption of gas molecules occurs on the film surface, where the gas acts as an electron acceptor. The removal of electrons from the film surface increases the number of holes (positive carriers), the main carriers in p-type materials, resulting in a decrease in the film's electrical resistance. This phenomenon is attributed to the change in surface charge density and the modification of the depletion region caused by the interaction between the adsorbed gas and the material surface [20].

As can be seen from Figs. 9–12, the sensor's resistance decreases with increasing operating temperature (50–150°C). This is attributed to the thermal excitation of charge carriers and the activation of surface interactions between gas molecules and the adsorbed oxygen species. These processes increase the concentration of charge carriers and reduce the potential barriers at the particle boundaries, leading to increased conductivity and decreased resistance [21].

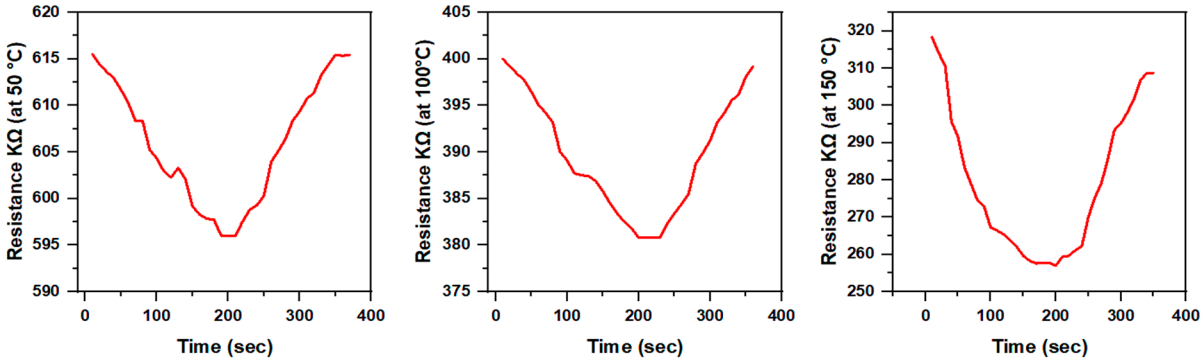

Figure 9: Resistance variation un-annealing at different operating temperatures against CO_2 gas.

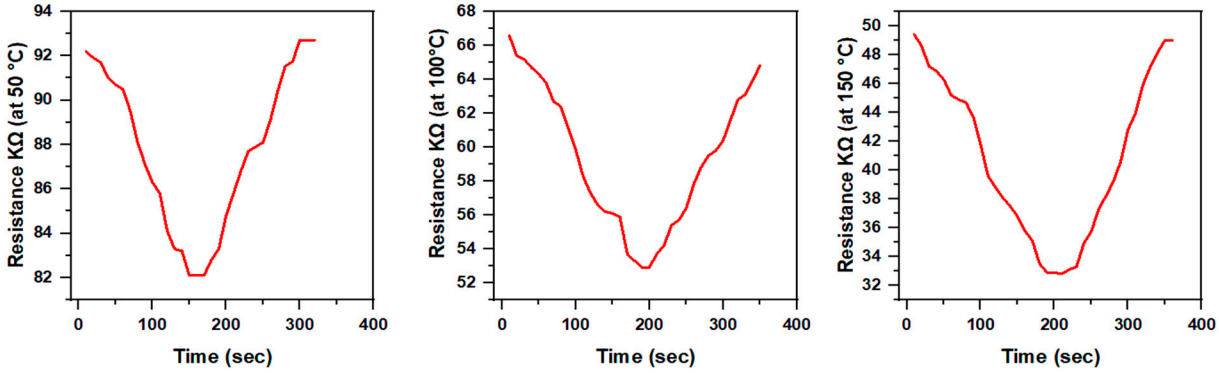

Figure 10: Resistance variation after annealing (200°C) at different operating temperatures against CO_2 gas.

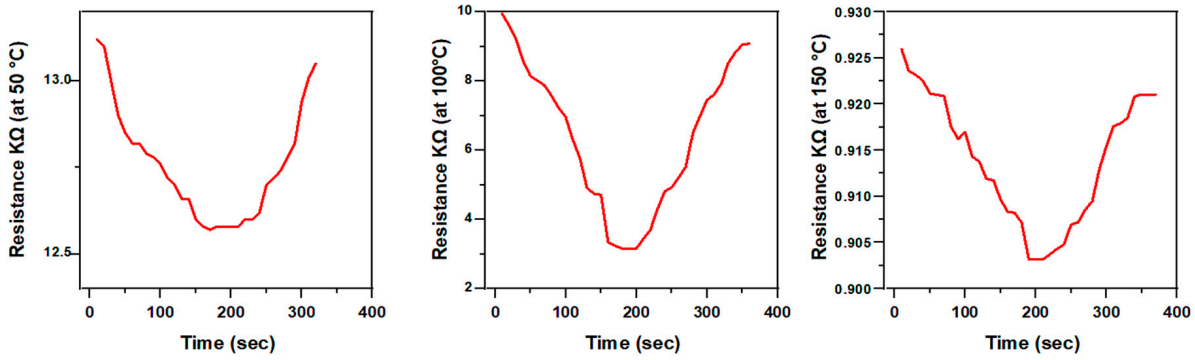

Figure 11: Resistance variation after annealing (300°C) at different operating temperatures against CO_2 gas.

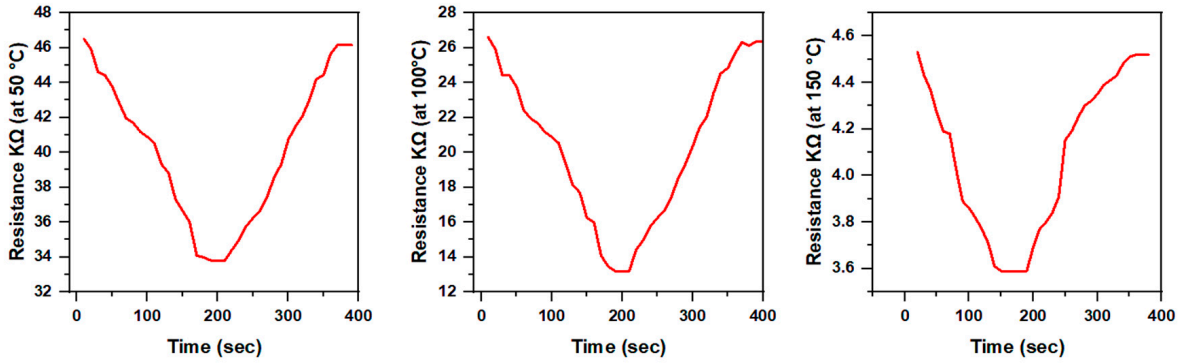

Figure 12: Resistance variation for after annealing (400°C) at different operating temperatures against CO_2 gas.

The sensitivity of SnS films was estimated by using the Formula (7) [22,23].

$$\left| S(\%) = \frac{Ra - Rg}{Ra} \times 100 \right| \tag{7}$$

In which *Ra* resistance in air, *Rg* the resistance in the presence of gas. It can be seen increasing sensitivity with increasing operating temp. The interactions between the sensor surface and gas determine the sensitivity regarding the tin sulfide sensor. Generally, increasing the operating temp. produces a more homogeneous surface with uniform roughness, resulting in a larger surface area and a higher possibility of gas reaction. Sensing is widely understood to be a surface process governed mostly by desorption and adsorption [24,25]. The sensitivity of membranes to CO_2 gas increases with increasing annealing temp. due to improved crystallinity and surface structure rearrangement, leading to reduced defects and enhanced charge transfer. Annealing at higher temperatures (400°C) promotes the formation of a more active surface with efficient adsorption sites, increasing the interaction of CO_2 with oxygen adsorbed on the surface and thus raising the S% value. Furthermore, achieving an optimal operating temperature (150°C at 400°C annealing) indicates a balance between the rate of gas adsorption and the rate of de-adsorption, which is essential for obtaining the highest response [26]. In general, improving the crystallinity and increasing surface stability through annealing enhances CO_2 sensitivity performance within a specific temperature range as shown in Table 2.

Table 2: Sensitivity of the SnS gas sensor upon exposure to CO_2 gas at different working temperatures.

Samp.	Operator Temp. (°C)	S%
Un-annealing	50	4.64
	100	7.1
	150	21
200°C	50	8.332
	100	25.29
	150	39.63
300°C	50	14.84
	100	74.98
	150	2.72
400°C	50	32.62
	100	56.79
	150	77.15

Fig. 13 shows the change in sensitivity of SnS films before and after annealing at different temperatures, along with changes in operating temperature. We observe that sensitivity generally increases with increasing operating temperature due to the activation of surface interactions between gas molecules and the oxygen adsorbed on the film surface. This leads to increased charge transfer within the material and improved sensitivity [22].

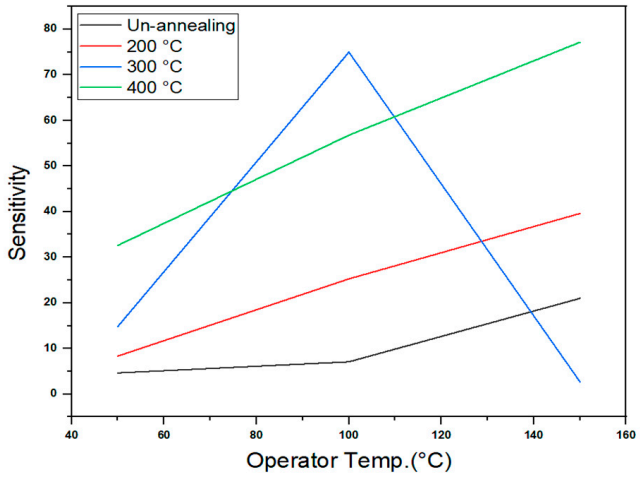

Figure 13: Variation of the sensitivity of the SnS gas sensor toward CO_2 gas at different operating temperatures.

4 Conclusions

The results confirmed the successful preparation of tin sulfide (SnS) thin films using thermal evaporation. X-ray diffraction (XRD) analysis revealed the formation of a rhombic crystalline phase, with a marked improvement in crystallinity after annealing. Scanning atom microscopy (AFM) showed an increase in surface roughness and an improvement in homogeneity, indicating that annealing contributed to defect reduction and enhanced grain growth. Optical studies showed strong absorption in the UV-Vis and visible ranges and higher transmittance at longer wavelengths, with the optical behavior significantly affected by the annealing temperature. Furthermore, the films exhibited a direct energy gap ranging from 1.35 to 1.62 eV, attributed to structural modifications resulting from annealing. Gas sensing tests demonstrated the p-type semiconductor nature of the films and a significant improvement in carbon dioxide (CO_2) sensitivity following annealing. The highest sensing response was obtained for the annealed membranes at 400°C, which were operated at 150°C, highlighting their suitability for carbon dioxide gas sensor applications.

Acknowledgement: The authors would like to thank the Department of Physics, College of Education for Pure Science (Ibn-Alhaitham), University of Baghdad, for providing laboratory facilities.

Funding Statement: The authors received no specific funding for this study.

Author Contributions: The authors confirm contribution to the paper as follows: study conception and design: Hawraa Hadi, Seham Hassan Salman; data collection: Sarmad Mahdi Ali, Dhufr Hadi; data analysis and interpretation: Seham Hassan Salman; manuscript preparation: Hawraa Hadi. All authors reviewed and approved the final version of the manuscript.

Availability of Data and Materials: The data supporting the findings of this study are available from the corresponding author upon reasonable request.

Ethics Approval: Not applicable.

Conflicts of Interest: The authors declare no conflicts of interest.

References

1. Norton KJ, Alam F, Lewis DJ. A review of the synthesis, properties, and applications of bulk and two-dimensional tin (II) sulfide (SnS). Appl Sci. 2021;11(5):2062. [CrossRef].
2. Hasan BA, Shallal IH. Structural and optical properties of SnS thin films. J Nano Adv Mat. 2014;2(2):43–9. [CrossRef].
3. Wongcharoen N, Gaewdang T. Influence of annealing temperature on the properties of SnS thin films prepared by vacuum thermal evaporation. Mater Sci Forum. 2017;890:295–8. [CrossRef].
4. Barote MA, Yadav AA, Masumdar EU. Effect of annealing on structural, optical and electrical properties of chemically deposited SnS thin films. Appl Surf Sci. 2011;257(16):7164–9. [CrossRef].
5. Patel M, Mukhopadhyay I, Ray A. Annealing influence over structural and optical properties of sprayed SnS thin films. Opt Mater. 2013;35(9):1693–9. [CrossRef].
6. Abdulah Zgair I, Mousa Al-Ogaili AO, Haneen Abass K. Influence annealing process on structural and optical properties of SnS thin films. J Kufa-Phys. 2023;15(2):13. [CrossRef].
7. Jain D, Jain G, Pal A, Agarwal S, Kumar S. Mixed phase formation of SnS-SnO_2 on air-annealed thermally evaporated SnS thin films. Thin Solid Film. 2023;780:139973. [CrossRef].
8. Khiera K, Hijri M, Radja I, Tudorache F, Guezzoul MH, Isik M, et al. Dual-functional Cu^{+}/Cu^{2+}-doped SnS thin films via spray coating: optoelectronic tuning and superior humidity sensor performance. J Alloys Compd. 2025;1039:183081. [CrossRef].
9. Hazem A, Mustafa MH. Influence of silver doping on the properties of sprayed cadmium telluride films. J Phys Conf Ser. 2025;3028(1):012048. [CrossRef].
10. Salman SH, Ali SM, Ahmed GS. Study the effect of annealing on structural and optical properties of indium selenide (InSe) thin films prepared by vacuum thermal evaporation technique. J Phys Conf Ser. 2021;1879(3):032058. [CrossRef].
11. Abbas IA, Hazaa SQ. Influence of annealing on the structural, morphology and optical properties of TiO_2 thin films. In: AIP conference proceedings. Melville, NY, USA: AIP Publishing LLC; 2020. p. 020037. [CrossRef].
12. Devika M, Reddy NK, Reddy KTR. Effect of annealing on the structural and optical properties of SnS thin films. Mater Chem Phys. 2006;98(2–3):305–8. [CrossRef].
13. Samani NK, Dehghani Z, Bioki HAA, Shayegh S. Annealing effect on structural and optical constants of SnS thin films for solar cells application. Optik. 2017;131:863–70. [CrossRef].
14. Sinsermsuksakul P, Sun L, Lee SW, Park HH, Kim SB, Yang C, et al. Overcoming efficiency limitations of SnS-based solar cells. Adv Energy Mater. 2014;4(15):1400496. [CrossRef].
15. Tanusevski A. Optical and electrical properties of SnS thin films. Semicond Sci Technol. 2003;18:501–5. [CrossRef].
16. Gunes I. Enhancing π-SnS thin films and fabrication of p-SnS/n-Si heterostructures through flow rate control in ultrasonic spray pyrolysis for improved photovoltaic performance. Appl Phys A. 2024;130(8):574. [CrossRef].
17. El-Nahass MM, Zeyada HM, Aziz MS, El-Ghamaz NA. Optical properties of thermally evaporated SnS thin films. Opt Mater. 2002;20(3):159–70. [CrossRef].
18. Hadi D, Hadi H, Salman SH. Effect of annealing on the physical characteristics of In_2O_3 nanoparticle films. Ann De Chim Sci Des Matériaux. 2025;49(3):315–20. [CrossRef].
19. Hadi H, Mohammed KA, Hadi D. Some physical properties of pure and Cu, Fe-doped CdS thin films. Int J Nanosci. 2022;21(4):2250031. [CrossRef].
20. Li Z, Li H, Wu Z, Wang M, Luo J, Torun H, et al. Advances in designs and mechanisms of semiconducting metal oxide nanostructures for high-precision gas sensors operated at room temperature. Mater Horiz. 2019;6(3):470–506. [CrossRef].
21. Gómez A, Martínez H, Calixto-Rodríguez M, Avellaneda D, Reyes PG, Flores O. A study of the structural, optical and electrical properties of SnS thin films modified by plasma. J Mater Sci Eng B. 2013;3(6):352–58. [CrossRef].

22. Shah MS, Ullah S, Tariq GH, Sahar MSU, Asghar G, Anis-ur-Rehman M. Thickness-dependent physical properties of tin sulfide thin films for an efficient sunlight-absorbing layer. J Electron Mater. 2022;51(11):6454–62. [CrossRef].
23. Yamazoe N, Shimanoe K. Theory of power laws for semiconductor gas sensors. Sens Actuat B Chem. 2008;128(2):566–73. [CrossRef].
24. Faisal MH, Salman SH. Effect of oxidation times on Gas sensitivity and characterization for (In_2O_3) thin films produced by thermal evaporated. J Phys Conf Ser. 2024;2857(1):012010. [CrossRef].
25. Salman SH, Jahil SS, Hassan NA, Abbas SA, Jasim KA. Ammonia gas sensing using porous silicon. J Phys Conf Ser. 2024;2857(1):012051. [CrossRef].
26. Alrazak AHA, Salman SH, Abbas IA, Mustafa MH, Ali HM, Abbas SA. Influence of doping with silver nanoparticles on the molybdenum trioxide gas sensor prepared by spray pyrolysis. Dig J Nanomater Biostruct. 2025;20(1):191–9. [CrossRef].